JOURNAL OF SOLID STATE CHEMISTRY 39, 7–14 (1981)

X-Ray Photoelectron Spectra and Electronic Structure of Rare-Earth Orthovanadates

M. V. RYZHKOV, S. P. KOSTIKOV, I. K. IVANOV, AND
V. A. GUBANOV

Institute of Chemistry, Ural Science Center, Academy of Sciences, Sverdlovsk, USSR

Received March 19, 1980; in revised form December 22, 1980

Photoelectron spectra of $4d$ and valence states in $R\text{VO}_4$ (R = Y, Nd, Eu, Gd, Tb, Dy, Yb) have been investigated. The experimental spectra are interpreted using the results of the $X\alpha$ discrete variational method calculations for orthovanadates. Transformations of electronic structure and covalency in the $R\text{VO}_4$ series are discussed. It is shown that lanthanide $4f$ orbitals significantly mix with the O $2p$ *A*O's and hybridize with the rare-earths $5p$ *A*O's. The $5p$ levels spin–orbital splitting in orthovanadates has been evaluated.

Introduction

X-Ray photoelectron spectroscopy provides interesting experimental data about the positions of energy levels, electronic structure details and their relative changes in the series of transition metal compounds. Quite many ESCA investigations for $3d$ and $4d$ element systems (*1, 2*) and some actinides (*3*) have been carried out recently; however, the number of papers on $4f$-metal compounds is very limited. XPS of rare-earth oxides R_2O_3 have been obtained by Orchard and Thornton (*4, 5*); but the authors interpret the results from the viewpoint of an ionic model of chemical bonding; i.e., the electronic states are treated as purely atomic. It seems to us, that such an approach leaves a number of aspects of electronic structure and spectrum band shifts unclear.

The rare-earth vanadates are of considerable theoretical interest. All of them possess the same zircon type of crystal lattice, but the population of $4f$ subshell for *RE* atoms changes drastically. Thus, this series of compounds allows us to study the interesting changes in covalent effects and chemical bonding depending on the number of $4f$ electrons at the *RE* atom. Moreover, these compounds show luminescent properties and are widely used in quantum optics, television tubes, and as the coating in luminescent lamps.

In the present paper, $4d$ and valence electron X-ray photoelectron spectra of rare-earth orthovanadates have been obtained and theoretical investigations of RVO_4, using the $X\alpha$ Hartree–Fock–Slater method, have been carried out.

Experimental

All the PE spectra were recorded on an HP 9270-1027 electron spectrometer using Al$K\alpha$ exciting radiation ($h\nu$ = 1487 eV).

0022-4596/81/100007-08$02.00/0

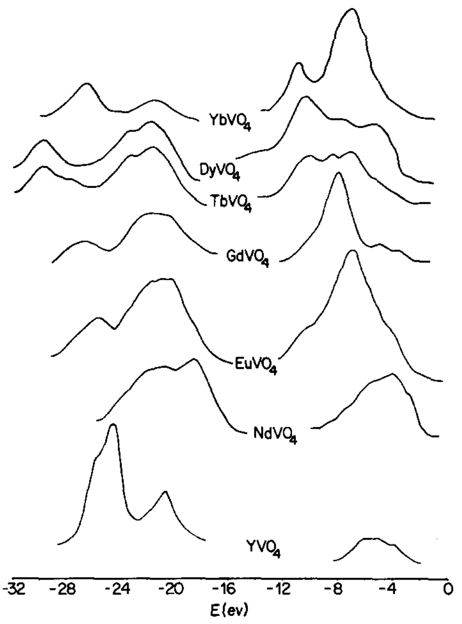

FIG. 1. Experimental X-ray photoelectron spectra of orthovanadates.

The powder samples were put in a vacuum of 5 × 10^{-10} Torr. The valence regions of the XPS were recorded from 0 to 20 eV and from 20 to 40 eV and then the results were combined. The spectral energies were corrected according to the work function of spectrometer ϕ_{sp}, the latter was measured relative to the carbon $1s^{1/2}$ = 284.5 eV level or Au $4f^{7/2}$ peak at 84.1 eV. The 4*d* electron spectra are rather complicated. This is partially due to the existence of unequivalent positions of a rare-earth atom in the *R*VO$_4$ lattice and impurities of other *RE* elements. The energy was measured with an accuracy of 0.2 eV. The valence band spectra are given in Fig. 1.

Computational Details

The calculations of RO_8^{13-} clusters (*R* = Y, Nd, Eu, Gd, Tb, Dy, Yb) in orthovanadates have been carried out by the spin-unrestricted discrete variation Xα method (*6, 7*) in the extended basis of numerical atomic orbitals. Geometrical structure of the clusters have been chosen from the literature (*8, 9*). The α coefficient was

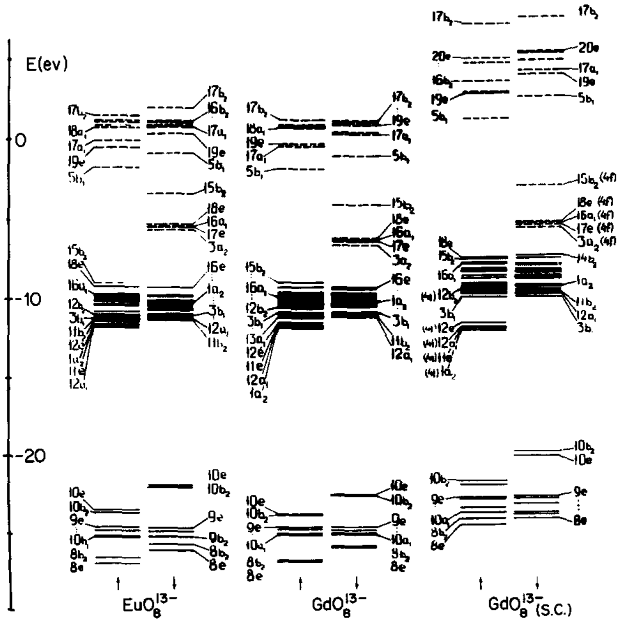

FIG. 2. Valence energy levels of EuO_8^{13-} and GdO_8^{13-} (non-self-consistent and self-consistent results) clusters.

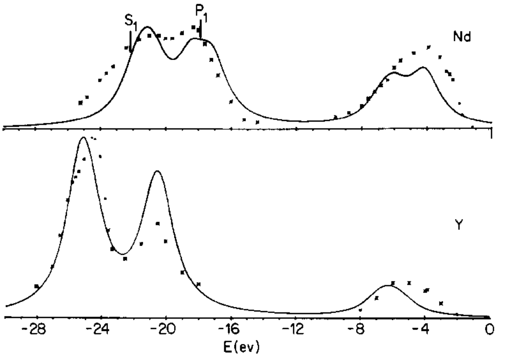

FIG. 3. Theoretical (solid line) and experimental (*) spectra of yttrium and neodimium orthovanadates. The P1 peak and S1 shoulder of theoretical spectra are due to 5*p* electron emission.

taken as the average of the atomic values (*10*). Approximate convergence of 0.1 eV was reached for the valence levels with 2000 points in the numerical integration procedure. The energy levels for $\mathrm{EuO_8^{13-}}$ and $\mathrm{GdO_8^{13-}}$ clusters are given in Fig. 2 as examples. The corresponding diagrams for other orthovanadates have been presented in another paper (*11*).

The information obtained on the energy levels structure permits one to calculate approximately the theoretical photoelectron spectra. The contribution of the *j*th molecular orbital to the photoelectron spectra can be expressed (neglecting two-center and off-diagonal elements (*2, 12*) as follows:

$$P_j = n_j \sum_i \sigma_i C_{ij}^2$$

where n_j is the degeneracy of the *j*th molecular orbital, C_{ij} are the coefficients in the LCAO expansion of the *j*th *MO* eigenvector, σ_i are the subshell photoionization cross sections. The values obtained by Scofield (*13*) have been taken as σ_i for yttrium, *RE*, and oxygen atoms. The *MO*'s calculated have been broadened by a Lorentzian function (*14–16*) with linewidth = 1.1 eV. Photoelectron spectra obtained using this procedure are given in Figs. 3–5.

Electronic Structure and Covalency Effects in Orthovanadates

The relative *MO* positions change very slightly from one cluster to another except for the rare-earth $12a_1$, $1a_2$, $11e$, $12e$, $15b_2$ molecular orbitals of 4*f* type (Fig. 2). The *MO*'s with energies in the interval −20 to −26 eV are of either ligand 2*s* or metal 5*p* character. Covalent mixing with other atomic orbitals is small as compared with the main contributions. Except for the mainly 4*f* *MO*'s mentioned above the levels with energies −15 to −5 eV are predominantly O 2*p* character with large *f*- and *d*-metal components (up to 20%). The series of vacant molecular orbitals with energies in the interval −2 to 3 eV are mainly composed of rare-earth 5*d*, 6*s*, and 6*p* orbitals with considerable admixtures of ligand orbitals. Core molecular orbitals keep their atomic character and their energies are close to corresponding atomic values.

The O 2*p* band width in $R\mathrm{O_8^{13-}}$ increases from Nd to Yb. The orbitals of oxygen 2*s* type in the lowest group of levels remain constant in the rare-earth series, the other *MO*'s of this group with the main 5*p* contributions become lower in energy and their polarization increases (11). The positions

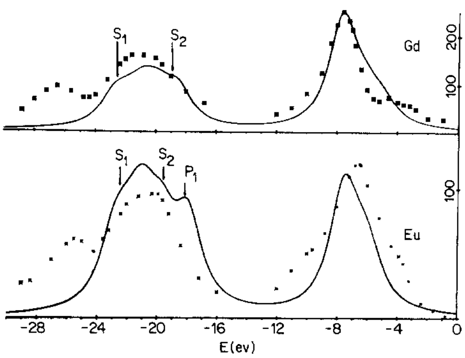

FIG. 4. Theoretical (solid line) and experimental (*) spectra of Eu and Gd orthovanadates. The P1 peak and S1, S2 shoulders are due to the 5*p* electron emission.

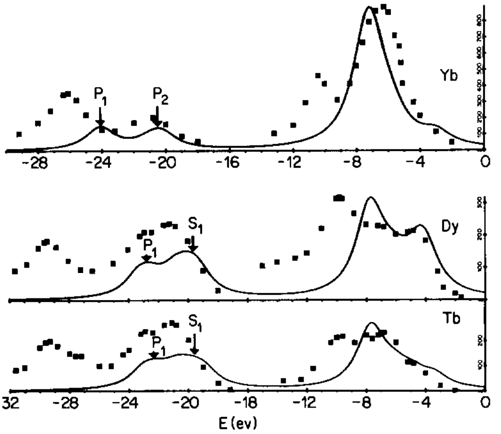

FIG. 5. Theoretical (solid line) and experimental (*) spectra of Tb, Dy, and Yb orthovanadates. The P1 peak and S1 shoulder are due to the 5*p* electron emission. The O 2*s* levels with corresponding P2 peak are separated from the 5*p* band (P1) for YbO_8^{13-}.

of highest vacant $5b_1$–$17b_2$ *MO*'s remain constant, even though their polarization changes significantly according to the number of unpaired 4*f* electrons.

The most striking changes in the cluster energy level diagrams are connected with the orbitals of predominantly 4*f* type (*11*). In the majority of orthovanadates (except $YbVO_4$), these orbitals for spin ↓ are located above the oxygen 2*p* levels and are composed of the narrow group of $3a_2 - 18e$ levels (the width is 0.3–0.4 eV) and $15b_2$ *MO*, situated ~1.7 eV (NdO_8^{13-})–3 eV (DyO_8^{13-}) above other 4*f* levels. The admixtures of oxygen 2*p* states to the different molecular orbitals mentioned above are of the same order. The 4f ↑ bands have the same structure and are located above oxygen 2*p* orbitals for $NdVO_4$ and below the ligand 2*p* bands (except the $15b_2\uparrow$ orbitals) for europium and other *RE* clusters. Thus, the total *f*-band width is ~1.7–3 eV for *RE* orthovanadates (this result is very unusual for Xα DV calculations of lanthanide compounds) in the calculations of cubic crystals EuO, EuS, CeO_2 (EuO_6^{10-}, EuS_6^{10-}, CeO_8^{12-} clusters) we have obtained the value for 4*f*-bandwidth ~0.4–0.16 eV (*17*), in cubic rare-earth oxyfluorides *R*OF (RO_4F_4 clusters of T_d^2 symmetry, *R* = La, Pr, Nd, Eu) the corresponding values are ~0.4–0.6 eV (*18*).

The calculations of orthovanadates discussed above were not iterated to self-consistency, and the fixed bases of neutral atoms were used. In order to check the influence of bases and self-consistency we have carried out the self consistent Xα DV calculation of the GdO_8^{13-} cluster with optimization of atomic orbitals, in which the ionic configurations resulting from successive iterations were used to generate the basis for new iterations. The results of this calculation are also presented in Fig. 2. There were no changes in the structure of 4*f* bands, the total band width remain constant at ~2.7 eV, the difference in the *MO* picture is the shift of ligands 2*s*, 2*p* levels, metal atom 5*p* and vacant states to higher energies. We can add that the results of *RE* orthophosphates calculations (the crystal structure is similar to the orthovanadate case) reveal the same width and structure of 4*f* bands (*19*).

Covalency effects analysis demonstrates that 4*f* *AO*'s noticeably mix with the ligand 2*p* orbitals and participate in chemical bonding. According to review (*20*), at the distance ~2 a.e. far from nucleus the value of the Pr 4*f* radial function is only 0.4–0.2 times lower than the maximum value (the results of Hartree, Hartree–Fock, and Hartree–Fock–Slater calculations). We have obtained ~0.26 times decrease for the europium 4*f* function at the same radius. Since the O 2*p* functions are ~0.5 times lower than their maximum value at the radius ~2.1 a.e. (*RE*–oxygen distances are ~4 a.e. in the orthovanadates), it is quite natural that the 4*f*–O 2*p* overlap populations are noticeable for elements of the beginning and center of the *RE* series and become small for the metals of the end of the lanthanide row. The atomic shells

TABLE I

AO POPULATIONS FOR RARE EARTHS IN ORTHOVANADATES

Atomic orbital	Cluster					
	NdO_8^{13-}	EuO_8^{13-}	GdO_8^{13-}	TbO_8^{13-}	DyO_8^{13-}	YbO_8^{13-}
4*f*	3.457	6.234	7.140	8.194	9.266	13.010
5*s*	1.997	1.998	1.998	1.998	1.998	1.998
5*p*	5.992	5.995	5.994	5.995	5.995	5.997
5*d*	1.057	0.996	0.945	0.946	0.847	0.874
6*s*	0.040	0.040	0.051	0.052	0.054	0.064
6*p*	0.054	0.054	0.061	0.061	0.062	0.068

populations in orthovanadates are given in Table 1.

Photoelectron Spectra of Orthovanadates

From the comparison of theoretical and experimental bands for YVO_4 it can be concluded that the region of the spectrum at energies from −30 to −18 eV is the result of Y 4*p* (peak in the vicinity of −25 eV) and O 2*s* (−20.5 eV) *MO* ionization. The excitations of oxygen 2*p*-type orbitals which contain some yttrium 4*p* *AO* covalent admixtures can be seen in the spectra region at −8 to −2 eV (the center is near −5.5 eV). There are also two bands separated by 6 eV in RO_8^{13-} spectra (Figs. 3–5). One can interpret the part of the spectrum with the energies −30 to −16 eV as a result of rare-earth 5*p* and oxygen 2*s* character levels ionization. The high-energy region in the orthovanadate spectra is the result of 4*f* and O 2*p* character *MO* contributions. According to Ref. (*13*), the rare-earth 4*f* orbital photoionization cross sections are one or two orders of magnitude larger than that of O 2*p* *AO*; thus the high-energy region of XPS depends on the positions of 4*f* type *MO*'s and 4*f* *AO* covalent contributions to O 2*p* *MO*'s only, i.e., the latter can be found in XPS just because of O 2*p* and *RE* 4*f* states hybridization.

The valence electron X-ray photoelectron spectra of RVO_4 are shifted to lower energy when increasing lanthanide atomic number and 4*f* *AO* populations. Theoretical spectra reveal the same trend; in addition, only rare-earth levels are displaced and the electron contribution, corresponding to the oxygen 2*s* and 2*p* states, remain nearly constant. From the present calculations, that is due to the energy lowering of 5*p* and 4*f* atomic states from Nd to Yb, which causes the decrease of corresponding *MO* energies. Since the spatial size of 5*p* *AO*'s is close to those of 4*f* *AO*'s, there is partial hybridization between them and the former is influenced by the different 4*f* *MO* populations.

Since the calculations presented here are nonrelativistic, the discrepancies between theoretical and experimental spectra for the 5*p*–2*s* band beginning from $EuVO_4$ are quite natural (*4, 21*). According to nonrelativistic and relativistic DV calculations of EuO (*22*) the energy of $5p^{3/2}$ and 5*p* (nonrelativistic version) is nearly the same and the energy gap between $5p^{3/2}$ and $5p^{1/2}$ is of the same order of magnitude as corresponding spin–orbital splitting for the free atom. This is confirmed by the comparison of theoretical and experimental spectra in the present paper (Figs. 4, 5). In addition, the energy separation between $4f^{5/2}$ and $4f^{7/2}$ *MO*'s in EuO has appeared to be small in comparison with 4*f* band splitting due to exchange polarization, crystal field, and covalency effects (*22*). We have attempted

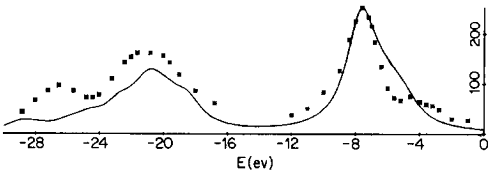

FIG. 6. $GdVO_4$ spectrum with $5p$ spin–orbital splitting included.

to include Gd $5p$ state spin–orbital splitting in the spectra calculation by the introduction of an extra band, assuming that $5p$ MO's with $j = \frac{1}{2}$ and $j = \frac{3}{2}$ are separated by the value $\Delta_{so} = 6.1$ eV obtained in free-atom calculations (*21*). Such a spectrum is given in Fig. 6. Perhaps the disagreement between the theory and experiment is the result of large splitting of $5p^{1/2}$ components of ↑ and ↓ spins. Moreover, the splitting between $5p^{1/2}$ and $5p^{3/2}$ levels in $GdVO_4$ appeared to be noticeably smaller than 6.1 eV. One can evaluate this parameter for gadolinium orthovanadate as ~5 eV, which is close to the corresponding Gd_2O_3 value ~4.7 eV (*4*). XPS permit one to evaluate Δ_{so} for $5p$ levels in orthovanadates: ~4.5 eV in $EuVO_4$ (in Eu_2O_3 is ~4.5 eV too), ~6 eV in $TbVO_4$ (~5.6 eV in Tb_2O_3), ~6.5 eV in $DyVO_4$ (~5.7 eV in corresponding oxide), ~5.3 eV in $YbVO_4$. The latter value is considerably smaller than that for Yb_2O_3 (~6.6 eV) (*4*).

We should like to consider a more detailed interpretation of $4f$ bands. The results of one-electron $X\alpha$ cluster calculations give the average energies of multiplets and do not permit an interpretation of multiplet structure of experimental spectra. Thus we have made an attempt to describe the $4f$ bands of $GdVO_4$, $TbVO_4$, $DyVO_4$, $YbVO_4$, using the atom-like method of "fractional parentage," treated by Cox (*23*) and Jorgensen (*24*), the energies of configurations, known from *RE* optical spectroscopy, were taken from Refs. (*20, 25*). The results of this interpretation are presented in Figs. 7, 8. The best agreement between atomic multiplets and the shape of $4f$ XPS is achieved for $YbVO_4$ (Fig. 7). According to this interpretation the double-peak structure of the experimental spectrum is due to electron emission of the same ↓ spin. However, the ratio between two peak intensities, deduced from calculation, differs somewhat from experiment. As far as *MO* calculation is concerned, we cannot use non-self-consistent $YbVO_4$ results for such an interpretation, because the initial cluster potential in first iteration corresponds to neutral atoms (i.e., the closed-shell $4f^{14}$ potential of Yb was used). From the comparison of experiment with either atomlike picture or molecular orbital treatment in $DyVO_4$ case (Fig. 7) one should identify the right peak at ~4.8 eV as due to the emission of a ↓ spin electron. It is easily seen that the group of multiplets, corresponding to spin ↑ excitations in the "fractional parentage" diagram is some-

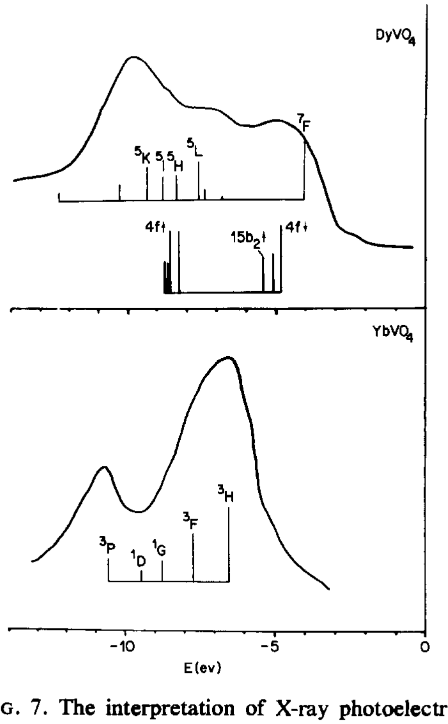

FIG. 7. The interpretation of X-ray photoelectron spectra of the $4f$ band region of $YbVO_4$ and $DyVO_4$.

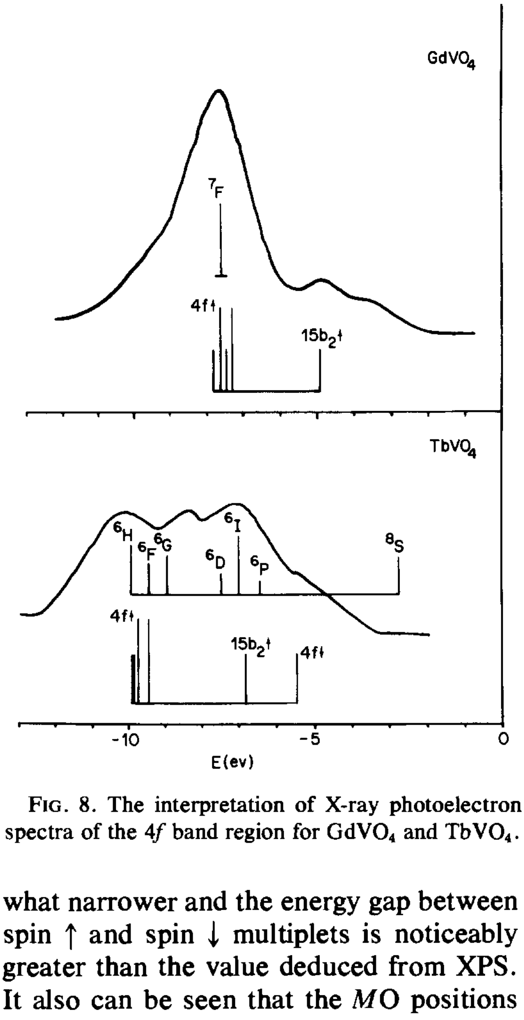

FIG. 8. The interpretation of X-ray photoelectron spectra of the $4f$ band region for $GdVO_4$ and $TbVO_4$.

what narrower and the energy gap between spin ↑ and spin ↓ multiplets is noticeably greater than the value deduced from XPS. It also can be seen that the *MO* positions for $DyVO_4$ agree with the average energies of both spin bands, and the position of $15b_2\uparrow$ orbital does not contradict the experiment. The atomlike multiplet structure for Tb is unacceptable for interpretation of $TbVO_4$ $4f$ XPS (Fig. 8), because of too large an energy difference between the ground ^8S state and other multiplets, corresponding to excitation of spin ↑ electrons. The width of the $4f$ band obtained from molecular one-electron energies is closer to experiment, and the position of $15b_2\uparrow$ orbital also does not conflict with the $TbVO_4$ spectrum. There is no multiplet structure for ionization of trivalent gadolinium atom (this fact was the reason for us to carry out the self-consistent calculation just for the $GdVO_4$ case), and the small peak at ~4.8 eV can be explained neither from a purely atomic point of view, nor as a contribution of O $2p$ states, because the Gd $4f$-band intensity has to be 70 times greater than that of the O $2p$ band (*13*). However, this peak is in good agreement with the position of the $15b_2\uparrow$ orbital in the *MO* picture.

Lanthanide $4d$ XPS have been obtained in the present paper too. These spectra have been recorded in quite a narrow interval (~15 eV) therefore the satellites, as reported in Ref. (*5*), have not been detected. Orthovanadate spectra line shapes are in good agreement with those of the main peak in Ref. (*5*). Both RVO_4 and R_2O_3 spectra demonstrate the increase of the $4d$ state binding energy from Nd to Yb. The positions of the level group center E_{4d} for corresponding clusters are given in Table II together with theoretical and experimental relative shifts of the E_{4d} value Δ_{th} and Δ_{ex}, respectively, while going from one rare earth to another. As seen from the table, theoretical and experimental results are in good agreement. Sharp increase of the Dy $4d$ binding energy in comparison with other lanthanides obtained by other authors (*5*) has not been confirmed in our work.

It is obvious that the present calculations are not perfect in several respects (relaxation effects and spin–orbital, and configuration interactions are neglected) and the interpretation obtained is mainly of qualitative character. However, the Xα discrete variational method used in this paper

TABLE II

$4d$ BAND CENTER ENERGIES AND THEORETICAL AND EXPERIMENTAL SHIFTS OF E_{4d} VALUE IN ORTHOVANADATES

	$NdVO_4$	$EuVO_4$	$GdVO_4$	$TbVO_4$	$DyVO_4$	$YbVO_4$
E_{4d}	−121.8	−139.8	−146.0	−152.1	−158.3	−183.1
Δ_{th}		18.0	6.2	6.1	6.2	24.8
Δ_{ex}		17.7	5.5	5.6	6.9	32.8

provides interesting information about electron structure characteristics and covalency effects in rare-earth orthovanadates. These calculations can be improved in several ways. First, transition state procedure (*26*) should be included in the calculation. Second, the consistent accounting of spin–orbital interaction in relativistic Xα DVM version (*27*) is necessary. However, at present the inclusion of relativistic effects together with the spin polarization is possible for quite simple systems only (*28*).

Acknowledgments

The authors are grateful to Dr. V. P. Zhukov for many helpful discussions.

References

1. V. I. Nefedov, "Stroenie Molecul i Chimicheskaya Svyas," Vol. 3. Viniti, Moscow (1975).

2. V. I. Nefedov, N. P. Sergushin, I. M. Band, and M. B. Trzhaskovskaja, *J. Electron Spectrosc.* **2**, 383 (1973).; V. I. Nefedov, N. P. Sergushin, Y. V. Salin, I. M. Band, and M. B. Trzhaskovskaja, *J. Electron Spectrosc.* **7**, 175 (1975).

3. B. W. Veal, D. J. Lam, H. Diamond, and H. K. Hockstra, *Phys. Rev. B* **15**, 2929 (1977).

4. A. F. Orchard and G. Thornton, *J. Electron Spectrosc.* **10**, 1 (1977).

5. A. F. Orchard and G. Thornton, *J. Electron Spectrosc.* **13**, 27 (1978).

6. F. W. Averill and D. E. Ellis, *J. Chem. Phys.* **59**, 6412 (1973).

7. D. E. Ellis and G. S. Painter, *Phys. Rev. B* **2**, 2887 (1970).

8. V. H. Schwarz, *Z. Anorg. Allg. Chem.* **323**, 44 (1973).

9. J. A. Baglio and O. J. Sovers, *J. Solid State Chem.* **3**, 458 (1971).

10. J. J. Rubin and L. G. Van-uitert, *J. Appl. Phys.* **37**, 2920 (1966).

11. V. A. Gubanov, D. E. Ellis, and A. A. Fotiev, *J. Solid State Chem.* **21**, 303 (1977).

12. U. Gelius, "Electron Spectroscopy" (D. Shirley, Ed.), North-Holland, Amsterdam/London (1972).

13. J. M. Scofield, *J. Electron Spectrosc.* **8**, 129 (1976).

14. V. A. Gubanov, A. Rosen, and D. E. Ellis, *J. Inorg. Nucl. Chem.* **41**, 975 (1979).

15. V. A. Gubanov, A. Rosen, and D. E. Ellis, *Solid State Commun.* **22**, 219 (1977).

16. V. A. Gubanov, A. Rosen, and D. E. Ellis, *J. Phys. Chem. Solids.* **40**, 17 (1979).

17. M. V. Ryzhkov, V. P. Zhukov, D. E. Ellis, and V. A. Gubanov, "Proceedings, International Symposium on The Physics of Actinides and Related 4*f* Materials, Zürich, Switzerland, April 9–11, 1980."

18. M. V. Ryzhkov, V. A. Gubanov, M. P. Byteman, D. E. Ellis, A. L. Hagström, and E. Z. Kurmaev, *J. Electron Spectrosc.* **21**, 193 (1980).

19. V. A. Gubanov and M. V. Ryzhkov, *Opt. Spectroscop.* **45**, 317 (1978).

20. K. N. R. Taylor and M. I. Darby, "Physics of Rare Earth Solids," Chapman & Hall, London (1972).

21. J. B. Mann and J. T. Waber, *At. Data* **5**, 201 (1973).

22. V. A. Gubanov, Doctor Chemical Science thesis, Novosibirsk, 1978.

23. P. A. Cox, "Structure and Bonding," Vol. 24, p. 59. Springer, Berlin/Heidelberg/New York (1975).

24. C. K. Jorgensen, "Structure and Bonding," Vol. 22, p. 49. Springer, Berlin/Heidelberg/New York (1975).

25. M. Campagna, G. K. Wertheim, and E. Bucher, "Structure and Bonding," vol. 30, p. 99. Springer, Berlin/Heidelberg/New York (1976).

26. J. C. Slater and K. H. Johnson, *Phys. Rev. B* **5**, 844 (1972).

27. A. Rosen and D. E. Ellis, *J. Chem. Phys.* **62**, 3039 (1975).

28. D. E. Ellis, *Int. J. Quantum Chem.*, 1977. (Quantum Chem. Symp. No. 1, 201.)